Chapter 2

GAS PHASE PRODUCTION AND LOSS OF ISOPRENE EPOXYDIOLS

Bates, K. H., J. D. Crounse, J. M. St Clair, N. B. Bennett, T. B. Nguyen, J. H. Seinfeld, B. M. Stoltz, and P. O. Wennberg (2014). "Gas phase production and loss of isoprene epoxydiols". In: *J. Phys. Chem. A* 118.7, pp. 1237–46. DOI: 10.1021/jp4107958.

Abstract

isoprene epoxydiols (IEPOX) form in high yields from the OH-initiated oxidation of isoprene under low-NO conditions. These compounds contribute significantly to secondary organic aerosol formation. Their gas-phase chemistry has, however, remained largely unexplored. In this study, we characterize the formation of IEPOX isomers from the oxidation of isoprene by OH. We find that *cis*- and *trans*-β-IEPOX are the dominant isomers produced, accounting respectively for 31 ± 5% and 66 ± 4 % of the IEPOX yield from low-NO oxidation of isoprene. Three isomers of IEPOX, including *cis*- and *trans*-β, were synthesized and oxidized by OH in environmental chambers under high- and low-NO conditions. We find that IEPOX reacts with OH at 299 K with rate coefficients of $(0.84 \pm 0.07) \times 10^{-11}$, $(1.52 \pm 0.07) \times 10^{-11}$, and $(0.98 \pm 0.05) \times 10^{-11}$ cm^3 molecule^{-1} s^{-1} for the δ1, *cis*-β, and *trans*-β isomers. Finally, yields of the first-generation products of IEPOX + OH oxidation were measured, and a new mechanism of IEPOX oxidation is proposed here to account for the observed products. The substantial yield of glyoxal and methylglyoxal from IEPOX oxidation may help explain elevated levels of those compounds observed in low-NO environments with high isoprene emissions.

2.1 Introduction

isoprene, a volatile organic compound (VOC) produced by deciduous plants, comprises the single most abundant atmospheric non-methane hydrocarbon by emission to the atmosphere, with estimates near 500 Tg C y^{-1} (Guenther *et al.*, 2006). The rapid oxidation of isoprene by OH radicals ($k = 1.0 \times 10^{-10}$ cm^3 molecule^{-1} s^{-1}) (Atkinson *et al.*, 2006) makes it an important driver in tropospheric chemistry, particularly in forested regions. When NO concentrations are sufficiently low, as is the

case in many areas with high isoprene emissions, isoprene oxidation can proceed by a HO_x-mediated (OH + HO_2) mechanism, which until recently was largely unexplored (Kuhlmann and Lawrence, 2004; Rosenstiel *et al.*, 2003; Wiedinmyer *et al.*, 2006). OH addition to isoprene, followed by O_2 addition and the peroxy radical + HO_2 reaction, leads to formation of isoprene hydroxyhydroperoxide (ISOPOOH) in yields exceeding 70% (Crutzen *et al.*, 2000; Lelieveld *et al.*, 2008; Ren *et al.*, 2008), with approximately 2.5% forming methacrolein (MACR) and 3.8% forming methylvinylketone (MVK) (Liu *et al.*, 2013; Navarro *et al.*, 2011).

Paulot *et al.* (2009b) showed that the reaction of ISOPOOH with OH forms isoprene epoxydiols (IEPOX) in yields exceeding 75% (Figure 2.1). The oxidation mechanism regenerates one equivalent of OH, partially accounting for the stability of HO_x levels observed in remote forested regions (Lelieveld *et al.*, 2008; Paulot *et al.*, 2009b; Ren *et al.*, 2008; Thornton *et al.*, 2002). IEPOX formation contributes to secondary organic aerosol (SOA) formation from low-NO_x isoprene oxidation, as its low volatility and high water solubility allow it to partition into the condensed phase (Lin *et al.*, 2012; Nguyen *et al.*, 2014a; Surratt *et al.*, 2010; Surratt *et al.*, 2006). Uptake of IEPOX onto acidic aerosol has been shown to contribute significantly to SOA in forested areas where anthropogenic pollutants (*e.g.* SO_2) are present (Zhang *et al.*, 2013). Estimates of global isoprene oxidation show that 95 ± 45 Tg C of IEPOX per year is formed globally, with the implication that the products of its subsequent reactions play a crucial role in tropospheric chemistry (Paulot *et al.*, 2009b).

Here, we report the relative yield of IEPOX isomers from isoprene oxidation, as well as the rate coefficients and products of their oxidation by OH. Using existing procedures with one significant novel enhancement, three isomers of IEPOX were synthesized. We then performed a series of individual experiments in which IEPOX isomers were oxidized by OH in an environmental chamber. Reaction rate coefficients of the IEPOX isomers were measured relative to propene. The lifetimes of δ1, *cis*-β, and *trans*-β-IEPOX against oxidation by OH (at 299 K and $[OH] = 1.0 \times 10^6$ molecule cm^{-3}, a typical atmospheric value) were found to be 33, 18, and 28 h, respectively. By comparing the isomers' retention times in a gas chromatograph (GC) connected to a chemical ionization mass spectrometer (CIMS) with that of IEPOX formed in situ by low-NO oxidation of isoprene, we show that *cis*- and *trans*-β-IEPOX account for the majority of IEPOX produced in the atmosphere, while the yield of δ1-IEPOX is small (<3%). These isomer ratios are consistent

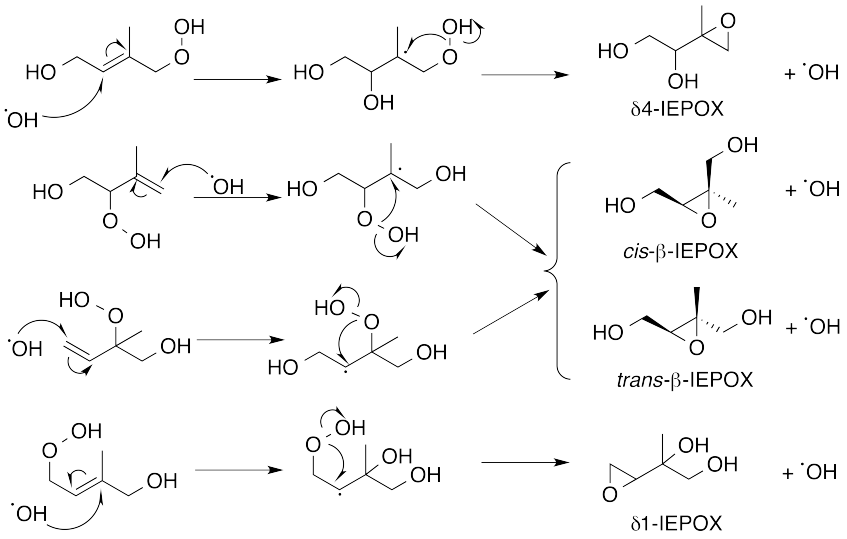

Figure 2.1: Mechanism for the formation of IEPOX from OH-initiated oxidation of ISOPOOH.

with the relative concentrations of their hydrolysis products (2-methylerythritol and 2-methylthreitol) observed in ambient aerosol (Claeys *et al.*, 2004; Ding *et al.*, 2008; Kourtchev *et al.*, 2005; Schkolnik *et al.*, 2005; Xia and Hopke, 2006; Zhang *et al.*, 2013). Additionally, experiments in the absence of propene were performed to determine the products of IEPOX oxidation by OH. Previous studies have inferred the products by a combination of theoretical models, observations of low-NO isoprene oxidation, and targeted chamber studies on IEPOX analogs (Paulot *et al.*, 2009a; Xie *et al.*, 2013). A more recent study measured the products of δ4 and *trans-*β-IEPOX oxidation by OH (Jacobs *et al.*, 2013). We observed a number of compound masses consistent with products predicted or detected in previous studies, for which we propose oxidative mechanisms. Differences in product yields between high- and low-NO conditions and between IEPOX isomers are described.

2.2 Experimental Methods

2.2.1 Synthesis

The IEPOX isomers used in these experiments were synthesized according to the procedures described by Zhang *et al.* (2012), with one significant change described below. All chemicals were purchased from Sigma Aldrich. The δ1- and *cis-*β-IEPOX used in photochemical oxidation experiments was 99% pure, as determined by NMR; the *trans-*β-IEPOX was >92% pure, and the impurity was not found to interfere with any part of the experiments.

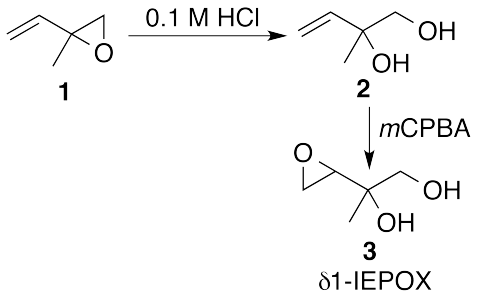

Figure 2.2: Reactions in the synthesis of δ1-IEPOX.

Briefly, δ1-IEPOX (2-(oxiran-2-yl)-propane-1,2-diol) was prepared from 2-methyl-2-vinyloxirane (**1**) as shown in Figure 2.2. The epoxide in compound 2 (0.98 g, 11.67 mmol) was first converted to the diol (**2**) by treatment with 0.1 M hydrochloric acid (10 mL), and the product was isolated by lyophilysis. The diol was then treated with *meta*-chloroperoxybenzoic acid (*m*CPBA, 4.25 g, 70%, 17.3 mmol) to afford δ1-IEPOX (**3**, 0.23 g, 1.9 mmol, 17% yield). The ^{1}H NMR spectrum (Figure 2.11 in the Supporting Information) matched previously published spectra (Zhang *et al.*, 2012).

Cis-β-IEPOX (*cis*-2-methyl-2,3-epoxy-1,4-butanediol) was prepared from 3-methylfuran-2(5H)-one, which in turn was prepared from citraconic anhydride (**4**) using procedures described by Nefkens *et al.* (1997) (Figure 2.3). Briefly, compound **4** (10 mL, 111.26 mmol) was treated with dicyclohexylamine (DCA, 25 mL, 122.4 mmol) in methanol to produce the DCA salt **5** (20.4 g, 62.7 mmol, 56% yield). Compound **5** was then treated with isobutyl chloroformate ($ClCO_2iBu$, 9 mL, 68.9 mmol) followed without purification by sodium borohydride ($NaBH_4$, 5 g, 132 mmol), to afford 3-methylfuran-2(5H)-one (**6**, 3.93 g, 40 mmol, 64% yield), which was purified by fractional distillation.

Conversion of compound **6** to 2-methyl-2-butene-1,4-diol (**7**) was adapted from procedures developed by Hoang *et al.* (2002), and was the only major change from the procedures of Zhang *et al.* (2012). The use of diisobutylaluminum hydride (DIBAL-H) instead of lithium aluminum hydride improved yields from 27% to 83%.

A flame-dried 100 mL round-bottom flask equipped with a stir bar was charged with compound **6** (1.63 g, 16.6 mmol, 1.00 equiv) and toluene (14 mL, 1.2 M) and lowered into a 0 °C bath (ice/water). DIBAL-H (neat, 4 mL, 22.4 mmol, 1.35 equiv) was added dropwise over several minutes. Once the addition was complete, the

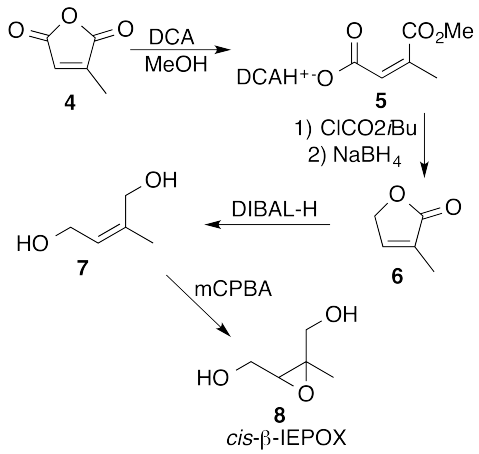

Figure 2.3: Reactions in the synthesis of *cis-β*-IEPOX.

bath was removed and the reaction was allowed to warm to room temperature. An additional portion of DIBAL-H (2.2 mL, 12.3 mmol, 0.74 equiv) was added after 1.5 h. TLC analysis at 3 h indicated no remaining starting material. Consequently, the reaction was lowered into a 0 °C bath and quenched with the dropwise addition of methanol (9 mL). The resulting mixture was diluted with toluene (14 mL) and water (3 mL), generating a large amount of solid that was broken up with a spatula. After 1.5 h of stirring, the reaction mixture developed into a biphasic suspension with no significant solids. $MgSO_4$ was added to the flask, and the reaction contents were filtered through a Celite/$MgSO_4$ column eluting with MeOH. The resulting organics were concentrated under reduced pressure, generating a white viscous oil. This oil was diluted with ethyl acetate (EtOAc) and again dried over $MgSO_4$, filtered, and concentrated under reduced pressure. The resulting crude oil was purified by flash column chromatography (SiO_2, 28 × 2 cm, 20% EtOAc in hexanes → 100% EtOAc) to afford compound **7** (1.40 g, 13.7 mmol, 83% yield) as a pale yellow oil. Compound **7** (0.33 g, 3.35 mmol) was treated with mCPBA (2.19 g, 77%, 9.8 mmol) according to the procedures of Zhang *et al.* (2012) to give *cis-β*-IEPOX (**8**, 0.16 g, 1.4 mmol, 42% yield). The ^{1}H NMR spectrum (Figure 2.12 in the Supporting Information) matched previously published spectra (Zhang *et al.*, 2012).

Trans-β-IEPOX (trans-2-methyl-2,3-epoxybutane-1,4-diol) was also prepared using procedures published by Zhang *et al.* (2012) (Figure 2.4). Briefly, 3-methyl-2-buten-1-ol (**9**, 4.7 g, 54.3 mmol) was treated with *tert*-butyldimethylchlorosilane (TBDMSCl, 9.9 g, 65.7 mmol) and diisopropylethylamine (Pr_2NEt, 10.5 mL, 60.3 mmol) to give compound **10** (7.92 g, 39.6 mmol, 73% yield). A hydroxyl group

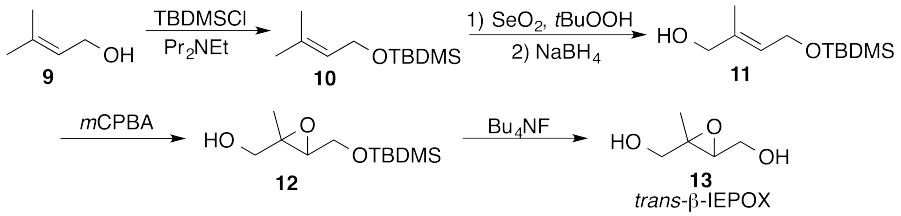

Figure 2.4: Reactions in the synthesis of *trans*-β-IEPOX.

was added to compound **10** in the *trans* position by treatment with selenium dioxide (SeO_2, 2.38 g, 21.5 mmol) and *tert*-butylhydroperoxide (*t*-BuOOH, 5.5 M in decanes, 8 mL, 44 mmol) followed without purification by reduction with sodium borohydride ($NaBH_4$, 1.36 g, 36 mmol) to give compound **11** (3.36 g, 15.5 mmol, 39% yield). Epoxidation with *m*CPBA (6.04 g, 77%, 27 mmol) yielded compound **12** (1.51 g, 6.5 mmol, 42% yield), and deprotection with tetrabutylammonium fluoride (Bu_4NF, 1 M in THF, 13.5 mmol) gave *trans*-β-IEPOX (**13**, 703 mg, 5.96 mmol, 92% yield). The ^{1}H NMR spectrum (Figure 2.13 in the Supporting Information) matched previously published spectra (Zhang *et al.*, 2012).

2.2.2 Gas Phase Experiments

Instruments and experimental procedures for gas-phase OH oxidation have been described in detail elsewhere (Paulot *et al.*, 2009b). Briefly, experiments were performed in a 0.85 m^3 fluorinated ethylene propylene copolymer (Teflon-FEP, Dupont) chamber at 299 K (± 2 K). Hydrogen peroxide (H_2O_2), at an initial mixing ratio of 2.5 ppm (± 10%), provided the source of HO_x for oxidation upon photolysis under UV lights. Each IEPOX isomer was oxidized in both high- and low-NO conditions (those in which the isoprene peroxy radicals react preferentially with NO or HO_2, respectively) with 570 ppb NO added for high-NO oxidation. Propene (125 ppb) provided the internal standard for OH concentration in experiments to determine the oxidation rate coefficient; in product studies, no propene was added.

The chamber was flushed with dry air and evacuated at least four times between successive experiments. In each experiment, IEPOX (30 ppb ± 50%, as measured by CIMS) was added to the chamber by spreading a single drop of the compound on the interior surface of a small glass cylinder and passing dry air through the cylinder into the chamber at 20 std L min^{-1}. Addition of δ1-IEPOX took 5 min per experiment; addition of *cis*- and *trans*-β-IEPOX took 30 min, and for *cis*-β-IEPOX the glass cylinder was heated to 60 °C in a water bath during addition to increase

volatility. H_2O_2 (~8.0 mg, 30% m/m in water) was added by the same method, for 10 min without heating. Propene gas was added by evacuating a 500 cm^3 glass bulb and filling it to ~11 Torr with propene, after which the bulb was back-flushed with N_2 to atmospheric pressure and pumped down to 11 Torr again. The contents were then flushed into the chamber by passing dry air through the bulb at 20 std L min^{-1} for 1 min. NO was added similarly, by filling the evacuated bulb to ~370 Torr with 1994 ± 20 ppm NO in N_2, and flushing the contents into the chamber for 1 min at 20 std L min^{-1}.

The chamber's contents were monitored throughout the experiment through a single sample line connected to five instruments: a time-of-flight chemical ionization mass spectrometer (ToF-CIMS, Tofwerk/Caltech); a triple quadrupole MS-MS CIMS (Varian/Caltech); a gas chromatograph with a flame-ionization detector (GC-FID Agilent 5890 II) to measure propene concentrations; a NO_x Monitor (Teledyne 200EU); and an O_3 monitor (Teledyne 400E). Both CIMS systems, which use CF_3O^- as the chemical ionization reagent gas, have been described in detail elsewhere (Crounse *et al.*, 2006; Paulot *et al.*, 2009b; St. Clair *et al.*, 2010).

Throughout the experiments, the ToF-CIMS monitored all *m/z* between 50 and 340 in negative-ion mode, while the MS-MS CIMS switched between scanning MS mode and tandem MS mode, to detect the fragmentation of IEPOX and its products and to resolve products of isobaric masses. All *m/z* signals are normalized to the reagent anion signal. IEPOX is monitored at *m/z* 203 (IEPOX+CF_3O^-) on both CIMS instruments and by *m/z* 203 → *m/z* 183 (IEPOX+CF_3O^-−HF) on the MS-MS CIMS in tandem MS mode. Photooxidation lasted approximately 3-7 h in each experiment. Nine gas-phase photooxidation experiments were performed, along with two experiments without oxidation to monitor loss of IEPOX to surfaces; details of the experiments are shown in Table 2.1.

Before and after photooxidation, monitoring by the five instruments described above was interrupted to separate compounds by gas chromatography before sampling by ToF-CIMS (GC-CIMS). One to three GC-CIMS runs were performed before and after each experiment. In each run, approximately 200 cm^3 of gas sample was cryo-collected on the head of an RPK 1701 column submerged in isopropanol chilled with liquid nitrogen (249 ± 3 K). The isopropanol bath was removed and the column was allowed to warm for 60 s before the GC temperature program was started (30 °C for 0.1 min, +3 °C/min to 60 °C, +10 °C/min to 130 °C, hold 3 min). Compounds eluted from the GC were ionized by CF_3O^- and monitored between *m/z* 50 and 340

expt #	IEPOX isomer	$[NO]_0$ (ppbv)	$[propene]_0$ (ppbv)	duration of photooxidation	experimental objective
1	*cis*-β	571	125	4:54:10	OH rate
2	*cis*-β	0	124	6:08:40	OH rate
3	*cis*-β	0	0	-	wall loss
4	δ1	0	126	5:58:30	OH rate
5	δ1	563	123	3:13:00	OH rate
6	*cis*-β	0	0	-	wall loss
7	*cis*-β	0	0	6:59:30	products
8	*cis*-β	570	0	7:01:30	products
9	*trans*-β	0	124	4:00:00	OH rate
10	*trans*-β	568	124	4:00:00	OH rate
11	*trans*-β	567	0	4:30:00	products

Table 2.1: Gas phase IEPOX experiments.

at a time resolution of 10 s^{-1}. Transmission through the GC varied between 60% and 70% for both IEPOX isomers, and was not statistically significantly different between the isomers. Further details regarding the GC-CIMS methodology will be provided in a forthcoming manuscript.

2.2.3 Determination of CIMS Sensitivity to IEPOX

The CIMS sensitivity to IEPOX was determined in four experiments, two each for *cis*- and *trans*-β-IEPOX, performed in the larger (24 m^3) Caltech environmental chamber. In each experiment, dilute (1-3 mM) aqueous solutions containing one IEPOX isomer and hydroxyacetone (as an internal standard) were atomized into the Teflon-FEP chamber for 2-8 h through a 15 cm perfluoroalkoxy Teflon transfer line. Temperature was ramped from 35 °C to 45 °C over the course of atomization to ensure minimal condensational losses. The measured weight of solution atomized allowed quantification of the moles in the chamber. During atomization, the mixing ratio of gas-phase IEPOX was monitored by negative-ion CIMS with a Varian triple quadrupole mass analyzer, described in greater detail elsewhere (St. Clair *et al.*, 2010). The instrument operated at 26.6 Torr and switched between scanning MS mode (*m/z* 50-250) and tandem MS mode, with unit mass resolution and 2-5 min time resolution. Dividing the CIMS normalized counts at *m/z* 203 (scanning MS mode) by the moles of IEPOX in the gas phase provided an estimate of the CIMS sensitivity. The dependence of IEPOX sensitivity on humidity was measured by adding various mixing ratios of water vapor to the CIMS during IEPOX detection.

No humidity dependence was detected. We find that the *cis*-β-IEPOX sensitivity is 1.8 times that of *trans*-β-IEPOX, consistent with the previously calculated ion-molecule collision rate ratio of 1.61 to 1 based on polarizability and dipole moments (Paulot *et al.*, 2009b).

2.2.4 Wall loss Experiments

Experiments were performed in both the 0.85 m^3 and 24 m^3 chambers to determine the extent to which the decay of IEPOX concentration with time could be attributed to loss to chamber walls. In both chambers, wall loss of IEPOX (~0.4% h^{-1}) was negligible compared to either loss by photooxidation or signal fluctuations due to temperature, except when nitric acid was injected to acidify the walls in the small chamber. The dramatic loss under acidic conditions is expected based on the sensitivity of the epoxide group in IEPOX to acid. Wall losses were accounted for in subsequent calculations of IEPOX photooxidation rates and products.

2.3 Results and Discussion

2.3.1 IEPOX + OH Rate Coefficients

Rate coefficients for the reaction of each IEPOX isomer with OH were calculated relative to that of propene with OH, for which the rate coefficient is well characterized; the value used in these calculations was 2.62×10^{-12} cm^3 $molecule^{-1}$ s^{-1} at 299 K (Atkinson and Arey, 2003a). A linear regression analysis of the natural log of the IEPOX concentration (normalized to the initial concentration) versus time over the course of photooxidation (Figure 2.5) gives a slope equal to the rate coefficient, k, multiplied by the concentration of OH. A similar regression can be performed for propene. The ratio of the two slopes is thus equal to the ratio of rate coefficients for oxidation of IEPOX and propene by OH, which allows for the calculation of the OH oxidation rate coefficient of IEPOX.

IEPOX + OH rate coefficients were calculated for each experiment with propene (Exp. 1, 2, 4, 5, 9, and 10), which included a high- and low-NO run for each of the three isomers. Propene concentrations were measured by GC-FID, and IEPOX concentrations by ToF-CIMS. Rate coefficients were then calculated using a linear regression method incorporating error in both dimensions, followed by an error-weighted mean (York *et al.*, 2004) of each isomer's runs. Rate coefficients determined in high- and low-NO experiments differed by no more than 19%, and the run-to-run differences did not correlate with NO level. Primary sources of error include fluctuations in temperature, which affect both oxidation rate coefficients and

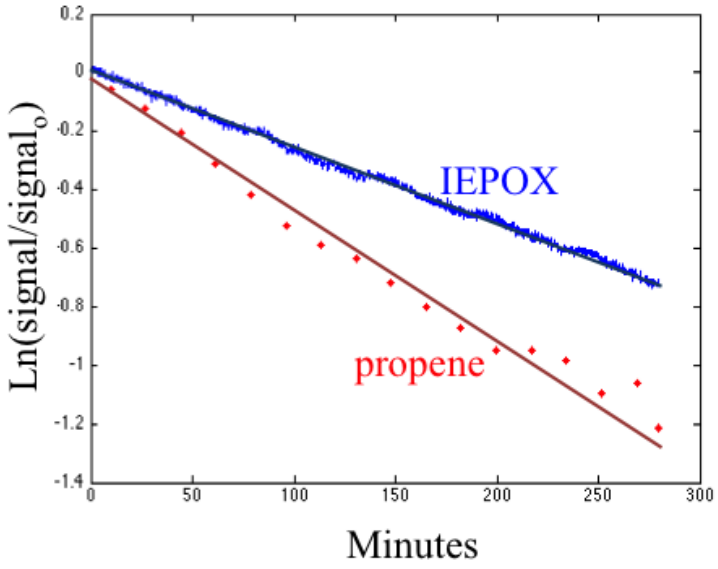

Figure 2.5: Decay of *cis*-β-IEPOX and propene in Expt. 1. The ratio of the slopes of propene and IEPOX concentrations over time (both on logarithmic scales) is equal to the ratio of the rate constants of each species' reaction with OH. Propene data are from GC-FID, while IEPOX data are from ToF-CIMS measured at *m/z* 203.

CIMS sensitivity to IEPOX, and the relative precision and frequency of GC-FID propene measurements.

Calculated OH oxidation rate coefficients and lifetimes for the three IEPOX isomers at ambient temperature are given in Table 2.2. *Cis*-β-IEPOX was found to react significantly faster than δ1 or *trans*-β-IEPOX with OH. The rate coefficients range from $(0.84 \pm 0.07) \times 10^{-11}$ cm^3 molecule^{-1} s^{-1} to $(1.52 \pm 0.07) \times 10^{-11}$ cm^3 molecule^{-1} s^{-1}, consistent with the value previously estimated as an upper limit by Paulot *et al.* (2009b) of 1.5×10^{-11} cm^3 molecule^{-1} s^{-1}. The only other study to have measured the OH oxidation rate coefficients of specific IEPOX isomers, by Jacobs *et al.* (2013), reported the rate coefficient of δ4-IEPOX + OH to be $(3.52 \pm 0.72) \times 10^{-11}$ cm^3 molecule^{-1} s^{-1} and that of *trans*-β-IEPOX + OH to be $(3.60 \pm 0.76) \times 10^{-11}$ cm^3 molecule^{-1} s^{-1}. These values are significantly higher than those reported here, and are inconsistent with the dynamics of the isoprene system studied by Paulot *et al.* (2009b) Clearly, further studies will be needed to resolve these differences.

isomer	rate (k)	$k_{low[NO]}$	$k_{high[NO]}$	lifetime (h)
δ1	0.84 ± 0.07	0.97	0.82	33.0 ± 2.8
cis-β	1.52 ± 0.07	1.40	1.62	18.3 ± 0.8
trans-β	0.98 ± 0.05	0.88	1.05	28.3 ± 1.4

Table 2.2: Rate coefficients for the reaction with OH of δ1, *cis*-β and *trans*-β-IEPOX. k is in units of cm^3 $molecule^{-1}$ s^{-1} $\times$ 10^{-11}, and lifetimes are for [OH] = 10^6 molecules cm^{-3}.

2.3.2 Relative Yields of IEPOX Isomers

Comparison of GC retention times of each IEPOX isomer to those of low-NO isoprene oxidation products reveals that *cis*- and *trans*-β-IEPOX are produced in much higher yield than δ1-IEPOX in the gas phase oxidation of isoprene by OH. These results are shown in Figure 2.6, in which *m/z* 203 (CF_3O^- plus IEPOX or ISOPOOH) normalized counts are plotted versus retention time for the three IEPOX isomers and for two time points in the low-NO oxidation of isoprene by OH, conducted under the same conditions as the low-NO IEPOX experiments detailed above. After 1 h, isoprene oxidation forms primarily two isomers of ISOPOOH, which appear on the GC-CIMS *m/z* 203 trace as two peaks centered at 12.5 and 13.3 min. After 10 h, some ISOPOOH remains, but two IEPOX peaks dominate, centered at 13.9 and 14.4 min. These correspond to *trans*- and *cis*-β-IEPOX, respectively. δ1-IEPOX also appears on the oxidized isoprene trace, but with a far smaller signal. The ratio of peak areas corresponding to δ1, *cis*-β, and *trans*-β-IEPOX is, respectively, 1 to 20.5 to 27.9.

While the CIMS sensitivity of δ1-IEPOX was not directly measured, previous calculations of molecular dipoles have determined that the sensitivity to δ1-IEPOX should be nearly equivalent to that of *cis*-β-IEPOX, and any deviation from this prediction is not expected to outweigh the large difference in peak areas between δ1-IEPOX and the other isomers. Thus, δ1-IEPOX is far less atmospherically relevant than the β-IEPOX isomers. δ4-IEPOX forms by a mechanism similar to that of the δ1 isomer, and likely has a similar retention time in the GC due to its analogous structure. No additional peaks were observed near the retention time of δ1-IEPOX that could have been assigned to δ4-IEPOX in the 10 h GC trace. Therefore, the δ4 isomer is expected either not to be formed or to co-elute with δ1-IEPOX, in which case the integrated peak area assigned to δ1-IEPOX accounts for the sum of the δ1 and δ4 isomers.

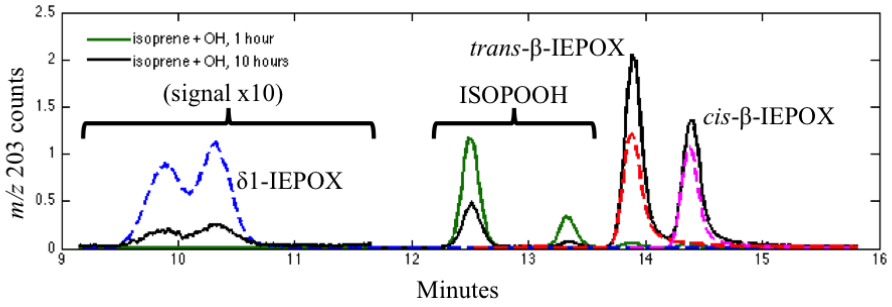

Figure 2.6: CIMS signals at *m/z* 203 from GC-CIMS chromatograms of δ1-IEPOX (blue), *cis*-β-IEPOX (pink), and *trans*-β-IEPOX (red) synthesized standards, as well as the *m/z* 203 products from OH-initiated low-NO_x oxidation of isoprene. The two major peaks seen after one hour of isoprene + OH oxidation (green) represent ISOPOOH, while the two major peaks seen after ten hours of oxidation (black) correspond with *cis*- and *trans*-β-IEPOX. The ten-hour signal is multiplied by a factor of ten between minutes 9.2 and 11.7, to show that a minor amount of δ1-IEPOX is formed. δ1-IEPOX appears as a double peak because the compound has two diastereomers.

Results from the sensitivity calibrations discussed above show that the single MS CIMS signal at *m/z* 203 is 1.83 times more sensitive to *cis*-β-IEPOX than *trans*-β-IEPOX. Scaling the signal areas by the sensitivity, we find that OH-initiated low-NO oxidation of isoprene produces concentrations of *cis*- and *trans*-β-IEPOX after 10 hours of oxidation in a ratio of 1 to 2.5 ($\pm$ 0.5). Part of this difference in concentrations can be explained by the faster reaction with OH of *cis*-β-IEPOX relative to *trans*-β-IEPOX. Using a simple kinetic model of isoprene, ISOPOOH, and IEPOX mixing ratios based on the signals observed in the low-NO oxidation of isoprene and the reaction rates calculated in the present study, we find the ratio of the yields of *cis*-β-IEPOX to *trans*-β-IEPOX produced from the reaction of isoprene with OH to be 1 to 2.13 ($\pm$ 0.30), and that *cis*-β and *trans*-β-IEPOX together account for >97% of observed IEPOX. The ratio of the *cis*- and *trans*- yields is similar to the ratio of 2-methyltetrol isomers found in SOA created by oxidation of isoprene by OH. Assuming that particle-phase hydrolysis of IEPOX proceeds by a typical acid-catalyzed mechanism as the evidence suggests (Eddingsaas *et al.*, 2010), in which protonation of the epoxide is followed by S_N2 attack by water, *cis*-β-IEPOX is expected to form 2-methylthreitol, while *trans*-β-IEPOX would form 2-methylerythritol. These 2-methyltetrol isomers have repeatedly been observed in isoprene-generated SOA in ratios of approximately 1 to 2, comparable to the ratio between *cis*- and *trans*-β-IEPOX we observe (Claeys *et al.*, 2004; Ding *et al.*, 2008;

Kourtchev *et al.*, 2005; Schkolnik *et al.*, 2005; Xia and Hopke, 2006; Zhang *et al.*, 2013).

2.3.3 Gas Phase Products of the Reaction of IEPOX with OH

Experiments performed in the 0.85 m^3 chamber in the absence of propene (Exp. 7, 8 and 11) were used to determine the products of gas-phase OH oxidation of *cis*- and *trans*-β-IEPOX. No product studies were performed on δ1-IEPOX due to its low atmospheric relevance. Mixing ratios of oxidation products were determined by multiplying the CIMS signal, normalized to the concentration of reagent ion in the chemical ionization region, by a calibration factor. For small, commercially available compounds, mixing ratio calibration factors were determined in previous experiments (Paulot *et al.*, 2009a). For larger products without authentic standards, instrumental sensitivities were assumed to be equal to those of their parent IEPOX isomer, as estimated in previous work based on polarizability and dipole moments (Paulot *et al.*, 2009a,b). Yields were then calculated by determining the slope of a simple linear regression between the mixing ratios of IEPOX and each product over the first 10-20 minutes of oxidation.

Time traces of oxidation products are shown in Figures 2.7 and 2.8, and first-generation product yields are given in Table 2.3. Reported uncertainties of yields account only for the standard deviations of the regressions, and do not include possible errors in calibration factors (estimated to be ± 30% for hydroxyacetone and glycolaldehyde and ± 20% for formic and acetic acid). Because these calibration factors have significant uncertainty and the CIMS sensitivity to IEPOX was not directly measured on the instruments used for these experiments, absolute yields cannot be accurately quantified, but yields can be compared between experiments. Additionally, because the yields reported in Table 2.3 are given as a percent of the IEPOX lost rather than as a percent of the total products observed, they do not necessarily add to 100%. Products lost to walls, products undetectable by our CIMS instruments, and uncertainty in sensitivity estimates all contribute to this deviation from carbon parity. We believe that uncertainties in the IEPOX and other large product sensitivity estimates account for the majority of error in the calculated yields, and for modeling purposes we suggest scaling the yields to a sum of 100%, knowing that significant uncertainties will persist until a more accurate determination of product yields can be measured.

The dominant small products of IEPOX oxidation detected by CIMS (Figure

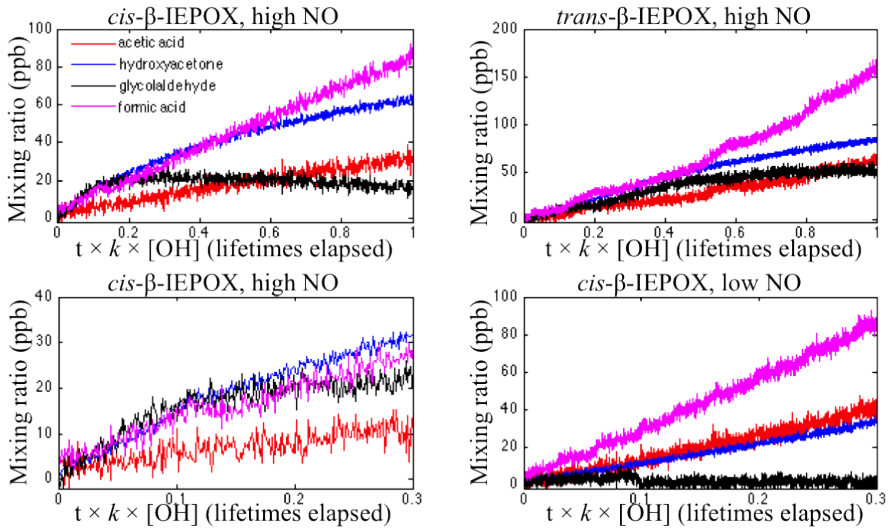

Figure 2.7: Time traces of dominant small products observed in the OH-initiated oxidation of *cis*- and *trans*-β-IEPOX: acetic acid (red), hydroxyacetone (blue), glycolaldehyde (black), and formic acid (magenta).

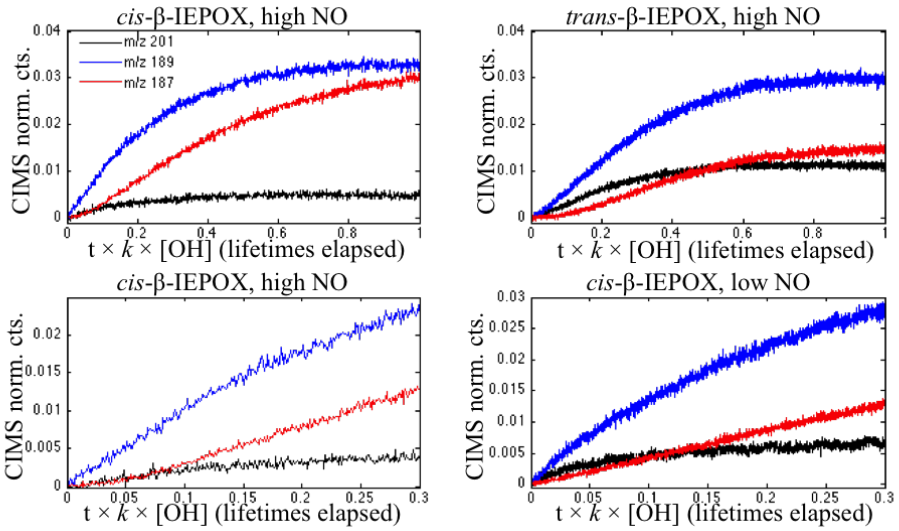

Figure 2.8: Time traces of dominant large products observed in the OH-initiated oxidation of *cis*- and *trans*-β-IEPOX as *m/z* 201 (black), 189 (blue), and 187 (red).

compound	sensitivity	yield (%)		
		cis-β-IEPOX high [NO]	*cis*-β-IEPOX low [NO]	*trans*-β-IEPOX high [NO]
m/z 201	variable	10.6 ± 0.7	12.9 ± 1.0	10.5 ± 0.27
m/z 189	variable	46.4 ± 1.7	37.1 ± 2.2	21.7 ± 0.5
m/z 187	variable	14.4 ± 0.6	10.4 ± 0.6	3.69 ± 0.15
glycolaldehyde	4.0×10^{-4}	11.8 ± 0.5	2.5 ± 0.6	4.55 ± 0.24
hydroxyacetone	3.8×10^{-4}	16.8 ± 0.3	8.5 ± 0.5	5.41 ± 0.17
acetic acid	2.3×10^{-4}	4.3 ± 0.3	7.8 ± 1.2	2.7 ± 0.3
formic acid	2.7×10^{-4}	15.8 ± 0.5	27.8 ± 2.1	8.8 ± 0.5

Table 2.3: First-generation yields of dominant products from the oxidation of *cis*- and *trans*-β-IEPOX. Sensitivities are in units of normalized counts per ppt in the CIMS flow tube, and the large products with "variable" sensitivities are assumed to have sensitivities equal to those of their parent IEPOX isomer (4.0×10^{-4} for *cis*-β-IEPOX and 2.2×10^{-4} for *trans*-β-IEPOX

2.7) were formic acid (FA, monitored at *m/z* 65 for FA·F^-), acetic acid (AA, *m/z* 79 for AA·F^-), glycolaldehyde (GLYC, *m/z* 145 for GLYC·CF_3O^-, corrected for AA·CF_3O^-), and hydroxyacetone (HAC, *m/z* 159 for HAC·CF_3O^-). Under high-NO conditions, both *cis*- and *trans*-β-IEPOX produced nearly equivalent first-generation yields of glycolaldehyde and hydroxyacetone. This matches previous speculation on the oxidation mechanism of IEPOX, such as those used in SAPRC-07 and MCM 3.2 (Carter, 2010; Saunders *et al.*, 2003). Both isomers also produced significant levels of formic and acetic acids, which had not been previously reported in IEPOX oxidation. Low-NO oxidation of *cis*-β-IEPOX resulted in diminished first-generation yields of glycolaldehyde and hydroxyacetone and elevated yields of acetic and formic acids relative to oxidation under high-NO conditions, suggesting a strongly NO-dependent mechanism for the formation of these small products.

The most prevalent C_4-C_5 products detected by CIMS (Figure 2.8) appeared at *m/z* 201, 189, and 187. Under high- and low-NO conditions, the two isomers gave nearly identical yields of the m/z 201 product. In contrast, *cis*-β-IEPOX produced over twice as much of the *m/z* 189 product as the *trans* isomer did, and nearly four times as much of the *m/z* 187 product. This evidence, along with differences in the yields of small products between the isomers, suggests a stark disparity between the oxidation pathways of the two isomers. We do not currently have an explanation for this difference, but ongoing computational studies are expected to shed light on this intriguing chemistry. Additionally, the appearance of significant amounts of large

products under high-NO conditions contrasts with the IEPOX oxidation mechanism used currently in photochemical models (*e.g.* MCM v3.2 and SAPRC07), in which IEPOX degrades quickly to form hydroxyacetone, glycolaldehyde, and other small products (Saunders *et al.*, 2003). Low-NO oxidation of *cis*-β-IEPOX produced slightly less of the *m/z* 189 and 187 products and slightly more of the *m/z* 201 product than under high-NO conditions, but the small magnitude of these changes suggests only a minor NO dependence of this oxidation pathway.

Proposed structures for the *m/z* 201, 189, and 187 compounds are shown in Figure 2.9. While many of these structures have been suggested previously as intermediates in the oxidative degradation of IEPOX, most have not yet been considered first-generation products, and their designation as such requires reconsideration of the mechanism for the first steps of IEPOX oxidation. We propose such a mechanism in Figure 2.10. We stress that this mechanism is neither complete nor certain, and it does not yet account for differing oxidation pathways between the two β-IEPOX isomers, nor for the formation of formic and acetic acids, but it improves upon existing mechanisms by incorporating both previous insights and the present results.

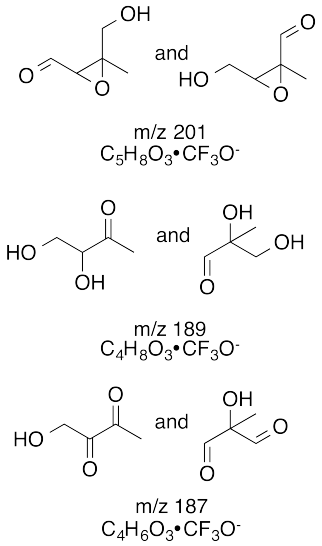

Figure 2.9: Proposed structures of the dominant large products observed in the OH-initiated oxidation of *cis*- and *trans*-β-IEPOX.

The mechanism begins with hydrogen abstraction by OH at the 1, 3, or 4 position. In the case of abstraction at positions 1 or 4, addition of O_2 and subsequent elimination of HO_2 gives the *m/z* 201 product, which accounts for ~10% of the first-generation pathway. Alternatively, a series of rearrangements can form a more

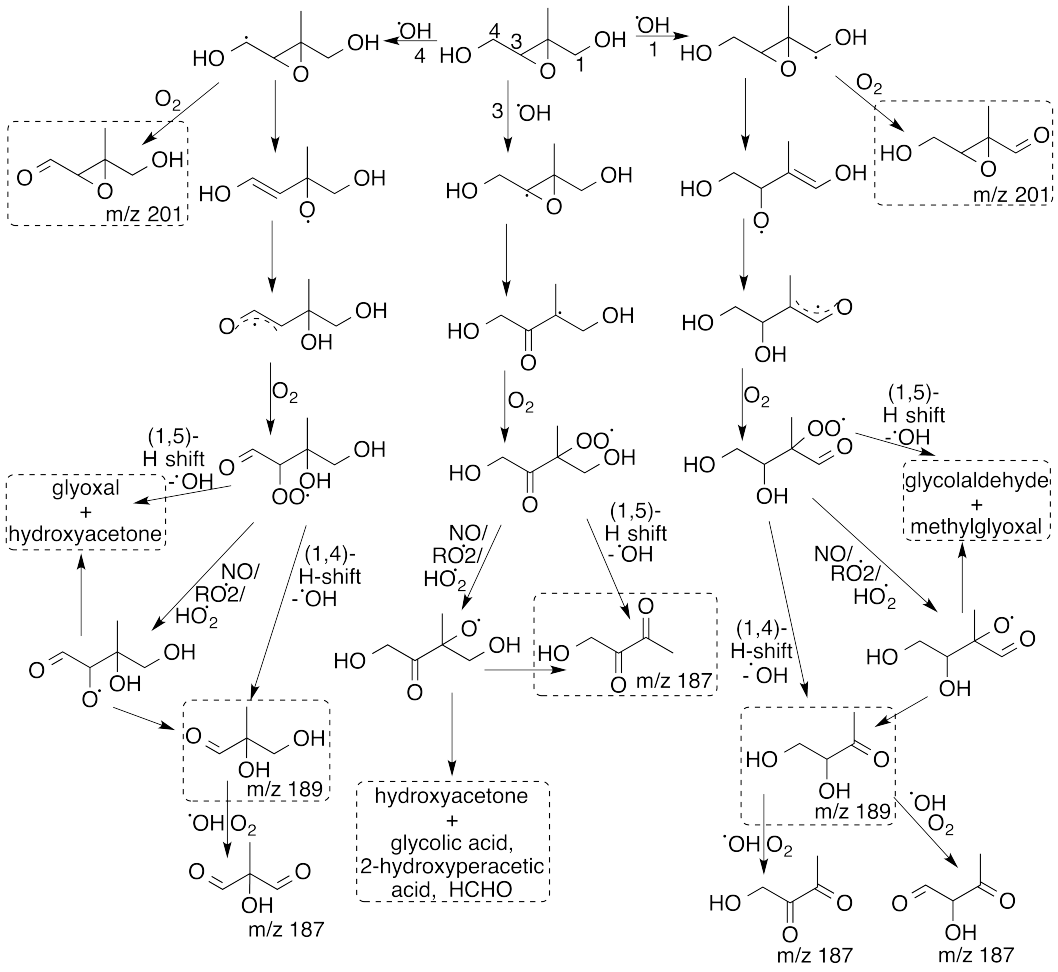

Figure 2.10: Proposed mechanism for the OH-initiated oxidation of β-IEPOX. Proposed first-generation products are outlined in dashed boxes.

stable alkyl radical prior to O_2 addition. The resulting peroxy radical can then undergo a variety of possible transformations. Reaction with HO_2, NO, or RO_2 to form the alkoxy radical results in fragmentation of the molecule, forming either a C_3 and a C_2 product or a C_4 product and CO. These pathways account for the formation of hydroxyacetone, glycolaldehyde, and the product detected at *m/z* 189. This mechanism also implies that glyoxal and methylglyoxal – neither of which can be detected by the CIMS instruments used here – are produced concurrently with hydroxyacetone and glycolaldehyde, respectively. Additionally, the peroxy radical can undergo unimolecular decomposition, *via* a 1,4-H shift from the α aldehyde or a 1,5-H shift from the α hydroxyl group, to form the same sets of products accessed by the alkoxy radical pathway. The product detected at *m/z* 189 can further react with OH and O_2 to form products detectable at *m/z* 187. Theoretically, the peroxy

radical could also react with HO_2 to form a hydroperoxide, or with NO to form a nitrate. Low product signal was observed at a mass consistent with the hydroperoxide (<5% under low-NO conditions), and almost no product was observed at a mass consistent with the nitrate (<1% under high-NO conditions), suggesting either that these reactions do not readily occur or that the non-volatile products are quickly lost to chamber walls.

In the case of hydrogen abstraction by OH at position 3, no product detectable at *m/z* 201 can be formed. Instead, isomerization and addition of O_2 leads directly to the peroxy radical, which can again undergo a 1,5-H shift with the α hydroxyl group and decompose to form a C_4 fragment. The C_4 fragment produced by the H-shift mechanism differs from those produced by abstraction at positions 1 and 4, and accounts for the first-generation yield of the product detected at *m/z* 187. Alternatively, the peroxy radical can react with HO_2, NO, or RO_2 to form the alkoxy radical, which decomposes to form either the same C_4 fragment or hydroxyacetone and a C_2 fragment. The C_2 fragment produced by this mechanism is expected to form glycolic or 2-hydroxyperacetic acids by reaction with HO_2 or decompose to formaldehyde (Saunders *et al.*, 2003). Low product signal was observed at masses consistent with the two acids (<2%). The sum of the yields of *m/z* 187 and hydroxyacetone provides an upper limit for the fraction of IEPOX + OH hydrogen abstraction that occurs at position 3, as hydroxyacetone can also be formed from other pathways. The yields reported in this study suggest that the first-generation formation of the *m/z* 189 products is the dominant pathway of IEPOX oxidation, and thus that hydrogen abstraction by OH occurs primarily at positions 1 and 4, but all pathways shown in Figure 2.10 contribute to the overall product breakdown of OH-initiated IEPOX degradation.

Many aspects of our proposed mechanism coincide with the one recently proposed by Jacobs *et al.* (2013) for *trans*-β-IEPOX, with the exception of our inclusion of the *m/z* 189 and 187 products, which they did not observe. Setting aside these compounds, the relative yields of hydroxyacetone, glycolaldehyde, and the *m/z* 201 product from *trans*-β-IEPOX oxidation are similar to those reported by Jacobs *et al.* (2013). Their study also shows products that our CIMS would observe at *m/z* 163, 217, and 235. With the exception of *m/z* 235, of which we detect small yields (<5%) with low statistical significance, these products are not observed in our experiments.

2.4 Conclusions

The recent discovery of IEPOX, and evidence of its importance as an isoprene oxidation product and SOA precursor, has led to widespread interest in its atmospheric fate. As IEPOX is estimated to account for a significant mass of global VOC (~100 Tg C y^{-1}), an understanding of its chemistry is critically important. The results presented here provide new insight into IEPOX behavior, which can be incorporated into chemical mechanisms of low-NO isoprene oxidation. The relative yields of IEPOX isomers as reported here, along with the OH oxidation rates of those isomers, serve to constrain the isomer distribution in the atmosphere, and explain the isomeric yields of 2-methyltetrols found in SOA. As differences in oxidation pathways between IEPOX isomers are elucidated, isomer abundances will further improve estimates of product yields.

The product studies conducted in this investigation largely corroborate existing predictions of the IEPOX oxidation pathway. Major products observed at *m/z* 189 and 187 fit with the existing MCM mechanism (Saunders *et al.*, 2003), although they notably appear as first-generation products rather than subsequent intermediates. Atmospheric observations of these products in high-isoprene, low-NO environments would test this finding. Yields of smaller products also generally match predictions, with the exception of formic acid, which has a much higher yield than currently predicted. However, differences in yields of most products between the two *beta*-IEPOX isomers suggest substantial divergence in the oxidation pathways for the two atmospherically dominant IEPOX isomers. Additionally, assuming glyoxal and methylglyoxal are co-products of hydroxyacetone and acetaldehyde in the oxidation of IEPOX, this chemistry is likely important in closing some of the disagreement between simulated and observed levels of these compounds in isoprene-rich environments (Myriokefalitakis *et al.*, 2008; Wittrock *et al.*, 2006). Although further studies incorporating measurements of glyoxal and methylglyoxal will be necessary to fully constrain the products of IEPOX oxidation, and to reconcile differences between our experiments and those of Jacobs *et al.* (2013), the products reported here provide a framework from which to improve existing models.

2.5 Supporting Information

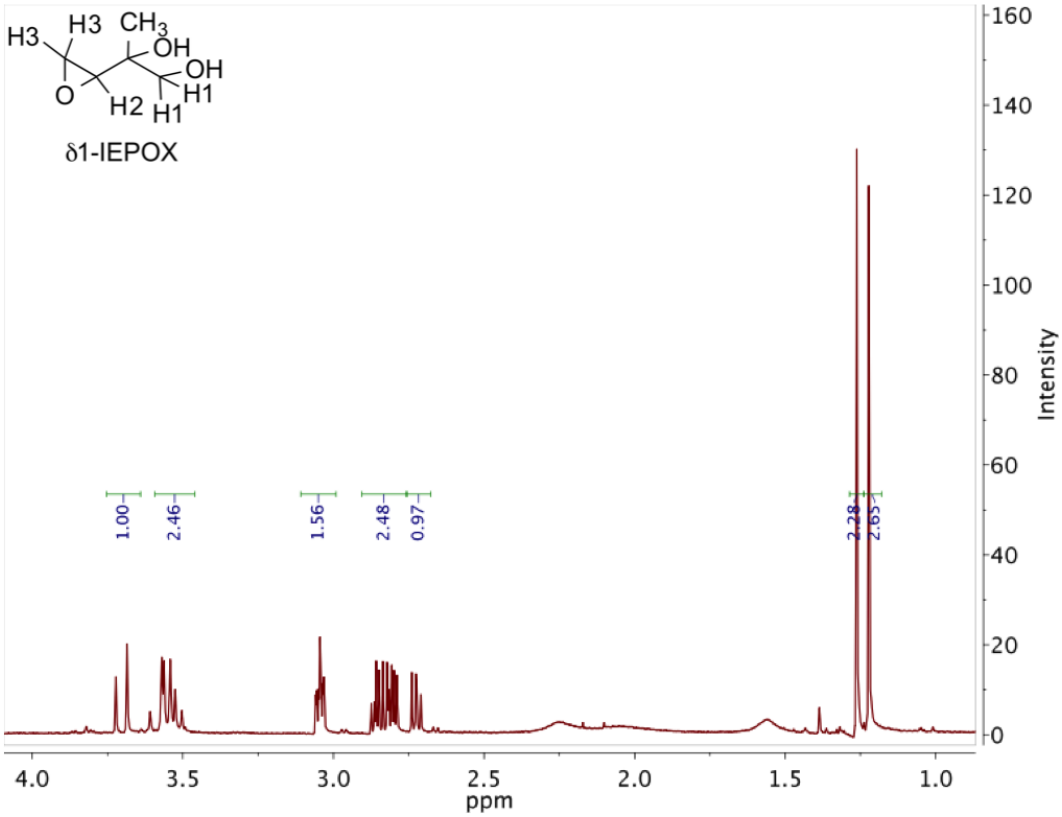

Figure 2.11: ^{1}H NMR (300 MHz, $CDCl_3$) of δ1-IEPOX.

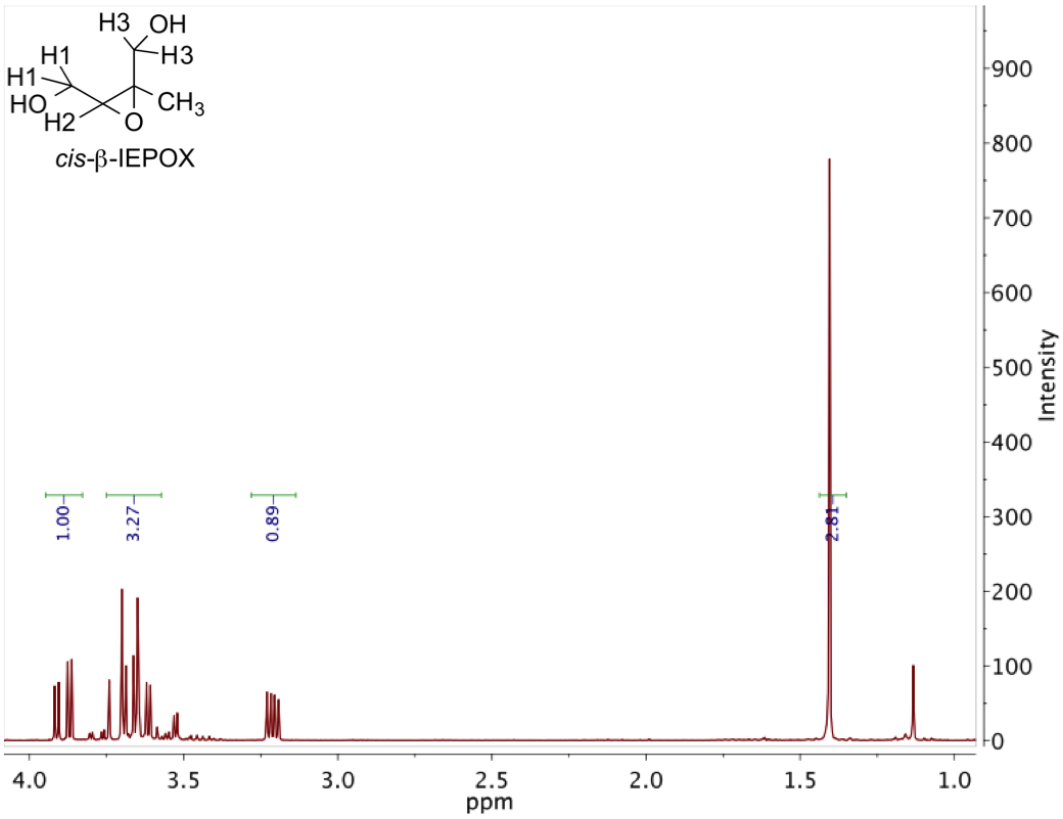

Figure 2.12: ^{1}H NMR (300 MHz, D_2O) of *cis-β*-IEPOX.

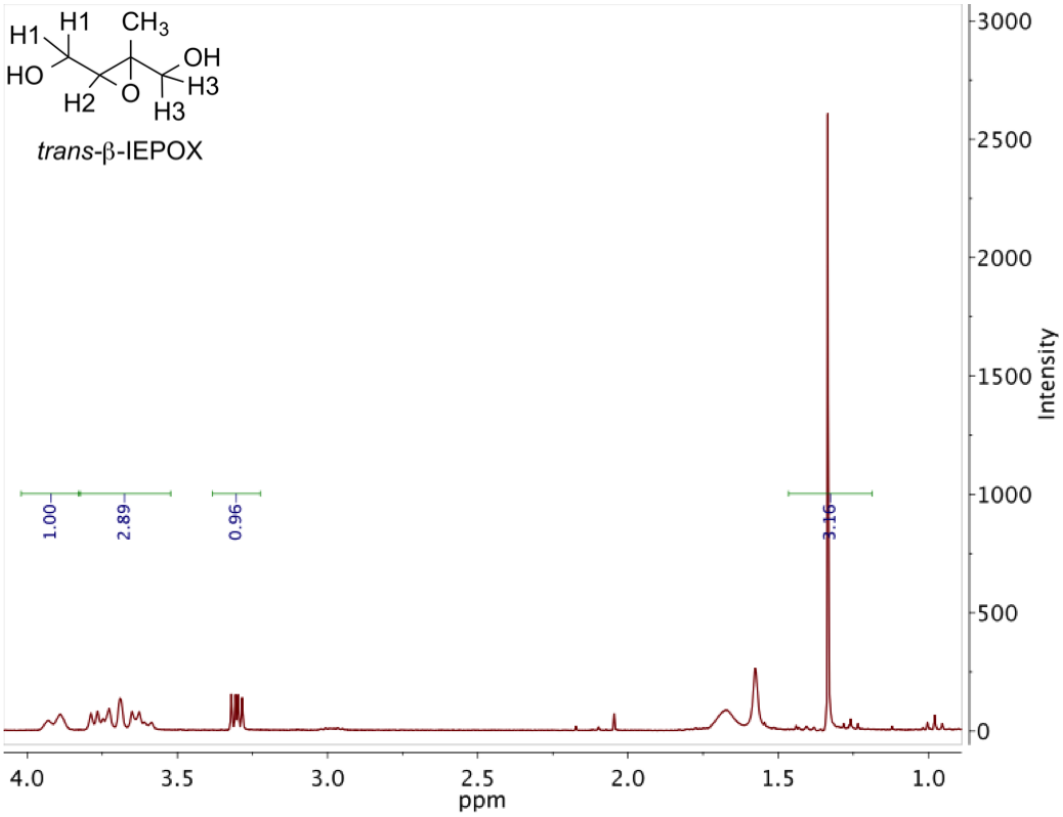

Figure 2.13: ^{1}H NMR (300 MHz, $CDCl_3$) of *trans-β*-IEPOX.